Title

Examination of axonal injury and regeneration in micropatterned neuronal culture using pulsed laser microbeam dissection

Journal

Lab on a Chip, 10(16)

ISSN

1473-0197

Authors

Hellman, Amy N

Vahidi, Behrad

Kim, Hyung Joon

et al.

Publication Date

2010

DOI

10.1039/b927153h

Published in final edited form as:
Lab Chip. 2010 August 21; 10(16): 2083–2092. doi:10.1039/b927153h.

Examination of Axonal Injury and Regeneration in Microfluidic Neuronal Culture Using Pulsed Laser Microbeam Dissection

Amy N. Hellman[a,b,c,*], **Behrad Vahidi**[d,e,*], **Hyung Joon Kim**[d], **Wael Mismar**[d], **Oswald Steward**[f], **Noo Li Jeon**[d,e], and **Vasan Venugopalan**[b,c,d,†]

[a] Department of Bioengineering, University of California, San Diego, La Jolla, CA 92093

[b] Department of Chemical Engineering & Materials Science, University of California, Irvine, CA 92697

[c] Laser Microbeam and Medical Program, Beckman Laser Institute, University of California, Irvine, CA 92697

[d] Department of Biomedical Engineering, University of California, Irvine, CA 92697

[e] Department of Mechanical & Aerospace Engineering, Seoul National University, Seoul 151-742, KOREA

[f] Reeve-Irvine Research Center for Spinal Cord Injury, University of California, Irvine, CA 92697

Abstract

We describe the integrated use of pulsed laser microbeams and microfluidic cell culture to examine the dynamics of axonal injury and regeneration *in vitro*. Microfabrication methods are used to place high purity dissociated central nervous system neurons in specific regions that allow the axons to interact with permissive and inhibitory substrates. Acute injury to neuron bundles is produced via the delivery of single 180 ps duration, λ=532 nm laser pulses. Laser pulse energies of 400 nJ and 800 nJ produce partial and complete transection of the axons, respectively, resulting in elliptical lesions 25 μm and 50 μm in size. The dynamics of the resulting degeneration and regrowth of proximal and distal axonal segments are examined for up to 8 h using time-lapse microscopy. We find the proximal and distal dieback distances from the site of laser microbeam irradiation to be roughly equal for both partial and complete transection of the axons. In addition, distinct growth cones emerge from the proximal neurite segments within 1–2 h post-injury, followed by a uniform front of regenerating axons that originate from the proximal segment and traverse the injury site within 8 h. We also examine the use of EGTA to chelate the extracellular calcium and potentially reduce the severity of the axonal degeneration following injury. While we find the addition of EGTA to reduce the severity of the initial dieback, it also hampers neurite repair and interfere with the formation of neuronal growth cones to traverse the injury site. This integrated use of laser microbeam dissection within a microfluidic cell culture system to produce precise zones of neuronal injury shows potential for high-throughput screening of agents to promote neuronal regeneration.

Introduction

Research in spinal cord injury and regeneration is hampered due to the lack of: (a) *in vitro* methods to produce precise and reproducible areas of injury for the study of axonal regrowth and (b) assays to evaluate the efficacy of chemicals that may provide axonal regeneration

[†]Correspondence: vvenugop@uci.edu.
[*]These authors contributed equally to this work

after injury. While numerous tools have been used to mimic CNS axonal injury *in vitro*, including the use of sharp metal blades[1], pulled glass electrodes[2], and rubber impactors controlled by electrically driven shafts[3], these procedures either require sophisticated computer-controlled micromanipulators or are limited to cutting only a few axons at a time which precludes high-throughput experimentation. In addition, these methods invariably violate the integrity of any supporting coating (e.g. collagen) which can hamper axonal regrowth[4].

While vacuum aspiration has been used successfully to sever isolated axons within a microfluidic culture platform and has facilitated quantification of both the pattern and the timing of axonal regeneration[5–8], this method lacks the precision necessary to determine important parameters, such as dieback of the proximal neuritic segment, and anterograde degeneration involving the distal neuritic segment. Acquisition of such information requires the ability to create reproducible zones of axonal injury with high-precision and high-throughput.

Pulsed laser microbeams have been used to produce axonal injury *in vivo* in animal models such as *C. elegans* and *Drosophilia*[9–12]. While these studies have been valuable, the injury and repair processes resulting from the laser microbeam irradiation have not been visualized. The vast majority of these studies have produced the axonal injury using multiple pulses of femtosecond laser radiation delivered at kHz or MHz repetition rates. Such lasers are attractive tools for cell microsurgery *in vivo* due to their ability to produce extremely localized damage zones in single cells[13,14]. However, the high cost and complex operation of these femtosecond laser systems makes them impractical for many researchers. Moreover, the high intensities associated with the use of ultrashort laser pulses likely produce photochemical effects such as the production of reactive oxygen species and direct chemical damage of biomolecules such as DNA[14]. An attractive alternative is the use of nanosecond and picosecond laser microbeams at visible wavelengths that provide much lower intensities that eliminates the possibility of photochemical damage. Moreover, such ns/ps laser microbeams can provide precise microdissection, are much simpler to operate, more reliable, and less costly than femtosecond lasers.

Here we demonstrate the creation of precise zones of axonal injury within a microfluidic neuronal culture platform[15] to examine the regeneration dynamics of axons as illustrated in Fig. 1. The creation of precise zones of axonal injury is enabled through the delivery of a single highly focused laser pulse (aka pulsed laser microbeam) that deposits energy with high spatial precision and provides a rapid, non-contact means for cellular manipulation.

In this study, we use 180 ps duration laser pulses to create reproducible and precisely controlled zones of axonal injury *in vitro*. To more closely model the *in vivo* microenvironment, we employ an established microfluidic based strip assay (Fig. 1) that utilizes substrate patterning to selectively place high purity dissociated central nervous system (CNS) neurons on a favorable substrate, while allowing only the axons to interact with permissive and inhibitory substrates presented in alternating strips. The microfluidic device provides reproducible results, is compatible with long-term culture of CNS neurons, and allows the manipulation of the ambient conditions[15]. We demonstrate the utility of this combined use of microfluidic and laser microbeam methods to study the initial dieback response and subsequent regrowth of CNS neurons in standard cell culture media, as well as in the presence of EGTA used to chelate extracellular calcium.

Materials and Methods

Cell Culture

Cortical neurons were prepared from embryonic (E18) rat embryos as described previously[16,17]. Briefly, cortexes of E18 rat embryos were dissected in calcium- and magnesium-free Hank's balanced salt solution (CMF-HBSS) containing 1 mM pyruvate, 4.2 mM sodium bicarbonate, and 0.3% bovine serum albumin, rinsed with CMF-HBSS, and incubated in a trypsin solution (0.125% trypsin in CMF-HBSS containing 0.5 mM EDTA) for 7 min at 37°C or for 25 min at ambient temperature. The addition of Dulbecco's modified Eagle's medium containing 10% fetal calf serum (FCS) is used to halt the trypsinization. The tissue was then triturated and centrifuged at 1000 rpm for 1 min. The resulting cell pellet was resuspended in 2 mL of Neurobasal medium containing 2% B27 supplement, 0.25% GlutaMax, and 1% penicillin-streptomycin (Invitrogen, Carlsbad, CA). The cell suspension was filtered through a 40 μm cell strainer and cell viability was determined using trypan blue.

Device Design and Fabrication

The patterning stamps were fabricated from poly dimethylsiloxane (PDMS) using replica molding and soft lithography[17]. Briefly, we used photolithography with a SU-8 negative photoresist (MicroChem Corp., Newton, MA) to fabricate a master mold with positive relief structures on a silicon wafer. We generated patterning stamps by casting a mixture of PDMS pre-polymer (Sylgard 184, Dow Corning, Midland, MI) and the curing agent on the master mold. After curing for 15 h at 70°C, we released the PDMS stamp from the master. The reservoirs were punched out, and the stamp was sterilized using UV light. The PDMS stamp contained two sets of channels, one for selective loading of the cells, and the other for patterning strips onto the surface. The sizes of strips were fixed: 25 μm wide channels separated by 25 μm spacings that were 10 μm deep. The stamps were then placed in reversible conformal contact with a patterned substrate to form the network of empty capillaries.

Patterned Substrate Preparation

With these microdevices alternating strips of Chondroitin Sulfate Proteoglycans (CSPG, Aggrecan, Sigma, St. Louis, MO) and poly-L-lysine (PLL) strips were created on 35 mm diameter glass bottom culture dishes (MatTek, Ashland, MA) using the Micromolding in Capillaries (MiMiC) method[18,19]. MiMiC consists of making confined channels by positioning the PDMS stamp in contact with a solid surface, and placing a drop of the solution containing the material to be patterned near the opening opposite the cell loading channel. The channels were filled by capillary action and the surfaces were patterned with proteins or materials.

Clean glass coverslips were first coated with sterile aqueous solution of 0.5 mg/mL PLL (MW=70–150 kDa, Sigma) in borate buffer overnight. The coated cover slips were rinsed in sterile water 3 times and air-dried for 30 min. The patterning stamp was placed over the PLL coated coverslips. Aggrecan was dissolved in distilled deionized water for a final concentration of 0.5 mg/ml. A pattern of alternating strips was formed by placing this aggrecan solution at the end of the patterning channels to allow it to completely fill the channels and dry for 1 h.

Cell Loading and Reduction of Extracellular Calcium

The neuronal cells were loaded into the microfluidic device via the circular inlets shown in Fig. 1 once the inhibitive molecules were patterned onto the substrate using an appropriately designed network of capillaries. Using the same PDMS stamp, neurons were selectively

placed adjacent to the strips by loading dissociated neurons in suspension to a channel located perpendicular to the strips. The cell-loading channel was 2 mm wide and 100 μm deep. A droplet (20 μL) of the cell suspension was loaded into the channel at density of 5×10^6 cells/mL. The cells were allowed to settle for ~1 hr to attach on the surface. The stamp was removed after extraction of most of the media. Using the circular inlets, the culture dishes were then flushed with neurobasal media to remove any nonadherent cells. The neurons were subsequently cultured in fresh media for 8–10 days prior to laser microbeam irradiation. The experimental groups consisted of 12–15 tracks, with each track containing a confluent bundle of axons.

To examine the process at low calcium levels, 6 mM EGTA was added to the culture media 1 h prior to laser microbeam irradiation. Standard neurobasal media has a calcium concentration of 1.8 mM and addition of 6 mM EGTA reduces the $[Ca^{2+}]$ to below 0.3 μM[20].

Pulsed Laser Microbeam Irradiation

An inverted microscope platform (Axiovert S100 2TV, Zeiss, Thornwood, NY) was used for laser microbeam irradiation and all assessments of cell culture. The microscope stage is enclosed and instrumented to provide a constant temperature of 37°C with 5% CO_2 to mimic physiological conditions and enable long-term experimentation. Cells remain viable on the microscope platform for over 24 h following laser microbeam irradiation. Laser axotomy is performed using a frequency-doubled Nd:YAG laser (SL332, EKSPLA, Vilnius, Lithuania) that provides 180 ps duration pulses at a wavelength of λ=532 nm. As shown in Fig. 2, the linearly polarized laser output is directed through a half-wave plate and polarization-sensitive beam splitter, followed by an iris to select the central portion of the laser beam. The beam emerging from the iris is directed into the rear microscope port and reflected upward into a microscope objective by a dichroic mirror placed in the microscope filter cube. The laser pulse energy is adjusted by rotating a linear polarizer inserted into the beam path. The laser pulse energy entering the rear entrance aperture of the objective was measured by removing the objective from the microscope turret and allowing the unobstructed beam to illuminate an energy detector (J3-05, Molectron, Portland, OR) set on the microscope stage. Pulse-to-pulse energy variation was ±3%. A 40×, 0.65 NA phase contrast objective (A-Plan, Zeiss, Thornwood, NY) is used for both the delivery of laser microbeam radiation to the neuritic bundle and phase contrast imaging. The precision of the laser microbeam irradiation allowed partial or complete transection of the individual neurite bundles using a single laser pulse energies of 400 nJ or 800 nJ, respectively. The adjacent tracks were uninjured and retained to serve as internal controls. Under strictly sterile conditions, neuritic injury was created at a distance of 75–100 μm from the cell body area, without adversely affecting the integrity of the PLL coating or disturbing the somata.

Time-Resolved Imaging

To examine the dynamics of the creation of the acute axonal injury we performed time-resolved imaging of the events immediately following the pulsed laser microbeam irradiation[21–24]. For these experiments, a 40× 0.8 numerical aperture brightfield objective (Achroplan, Zeiss, Thornwood, NY) was used for the delivery of the laser microbeam irradiation as well as the subsequent imaging. Illumination for the time-resolved images was provided by delivering a short light pulse at the desired time delay following the arrival of the Nd:YAG laser pulse at the sample. The polarized beam splitter divides the beam into low- and high-energy beam lines. The high-energy beam line is focused into a glass cuvette containing a fluorescent dye (LDS 698, Exciton Inc., Dayton, OH) that is excited by the λ_{ex} = 532 nm laser pulse and emits light at λ_{em} = 698 nm. The dye cell emission is focused into a 600-μm-diameter multimode optical fiber (UMT 600, 0.39 NA, Thor Labs, Newton, NJ)

with the fiber output being directed into the microscope condenser to illuminate the sample for time-resolved imaging. Different lengths of optical fiber are used to adjust the arrival time of the fluorescent emission relative to the arrival of the low-energy beam line at the sample. The maximum delay time for the fiber-optic delay line is 2000 ns. For longer delay times, illumination is provided by a flash lamp electronically triggered by the laser. The images are captured by an I-CCD camera (PI-MAX 512, Princeton Instruments, Trenton, NJ) using an exposure time of 0.5 ns when using the dye cell emission for illumination and to 200 ns when using flash lamp illumination. A long pass filter (LP 570, Edmund Optics, Barrington, NJ) was used to prevent scattered laser radiation from reaching the camera. This system allowed us to irradiate and image the sample at time delays of 0.5 ns to 10 μs required to capture the full dynamics of process of acute axonal injury.

Time-Lapse Microscopy and Image Analysis

To examine the subsequent response to the acute axonal injury, images were taken by a CCD camera (Quantix, Photometrics, Tuscon, AZ). Camera operation and image acquisition was controlled using WinView32 imaging software (Princeton Instruments, Trenton, NJ). Images were acquired immediately before and following laser microbeam exposure, and monitored at 1 min intervals for up to 8 h. This enabled observation and measurement of the neurite response, including lesion size and distances of neuritic dieback, anterograde degeneration, and regeneration. Images were compiled and intensities adjusted using Image J software.

Results

Time-Resolved Imaging of Acute Laser Microbeam Induced Injury

Our previous studies have utilized highly focused laser microbeam irradiation to achieve targeted lysis of adherent and suspension cells in both standard Petri-dish and microfluidic environments[21–24]. In these studies, we demonstrated that the delivery of a pulsed laser microbeam to adherent cells results in the formation of a laser-induced plasma followed by the emission of a pressure shock wave and cavitation bubble formation, expansion, and collapse[21,22,25]. For laser pulses of nanosecond and picosecond duration, this entire cascade of processes occurs on the microsecond time scale. The studies have established that cellular injury is due to direct vaporization by the plasma combined with the mechanical shear stresses associated with the cavitation bubble expansion and/or collapse[21–25].

We employed time-resolved imaging to visualize the cavitation bubble interaction with the axon bundles and confirm this process as the mechanism responsible for axonal injury. Figure 3 is a time-resolved image series of the shock wave and cavitation bubble dynamics resulting from a 180 ps duration, 400 nJ laser microbeam exposure. In Figs. 3(a) and 3(b), the shock wave can be seen and quickly passes out of the field of view and does not appear to create any axonal damage. Close inspection of Figs. 3(d), 3(e), and 3(f), reveals that the severing of axons occurs within the first microsecond following laser microbeam irradiation. In Fig. 3(d), axons can still be seen under the bubble. In Fig. 3(e) the first sign of axonal damage appears and in Fig 3(f), no axons can be seen in the center of the bubble, indicating that the axons have been severed. The axon bundles can be seen near the edge of the bubble. This time scale for axonal injury is consistent with our previous studies of laser microbeam-induced lysis of adherent cells that demonstrated cellular injury to occur during cavitation bubble expansion when the laser microbeam focal volume is placed 10 μm above the cell surface[22,23].

Axonal Response to Partial and Complete Transection in Standard Media

The delivery of laser pulses at λ=532 nm with 180 ps duration produced localized axonal injury to 25-μm-wide axon bundles *in vitro*. Fig. 4a shows the lesion produced by the irradiation of the axon bundle with a single 180 ps, 400 nJ laser pulse. The irradiation produces an elliptical lesion <25 μm in width in the targeted bundle, while the neighboring bundle situated 25 μm away was unaffected. Increasing the laser pulse energy to 800 nJ provided complete transection of the axon bundle, as shown in Fig. 4b. This higher energy level also produced damage in the adjacent axon bundle (note the 3 blebs in upper bundle in Fig. 4b).

Fig. 5 provides a series of time-lapse images following partial laser axotomy created in a 25-μm-wide axon bundle using a single 400 nJ pulse, resulting in an elliptical defect ~25 μm across (Fig. 5b). Neurite dieback begins immediately following the neurite transection and the length of dieback in both the proximal and distal sections of the neurite bundles was quantified. As the axons die back, the axon tips form characteristic enlargements (retraction balls) that are evident in the images and identified by the arrows in both the proximal (left) and distal (right) segments of the transected neurons in Fig. 5c. Within 1–2 h post-injury, distinct growth cones emerge from the proximal neurite segments (arrow, Fig. 5d). The distal neurite segments dieback and show evidence of degeneration as early as 1 h following injury. The degenerating distal neurites continue to withdraw from the injury site and display some blebbing but pose no barrier to the growing front of regenerating axons. Within 3–5 h, a uniform front of regenerating axons are seen to begin crossing the injury site, with one axon crossing over the site of the laser irradiation (arrow, Fig 5e). This pattern of regeneration with no regrowth in the non-aggrecan coated areas is a strong indicator that the laser pulse does not violate the integrity of the underlying surface coating, and facilitates axonal regeneration across the site of injury. At 5 h, several axons had traversed the area of injury. Several cultures were followed for as long as 3 days following injury by which time the distal neurites completely detached from the matrix bed and were seen floating in the culture medium. By contrast the regenerating neurites remained on the tracks, with no remnants of the degenerated distal neuritic fibers.

Fig. 6 provides a series of images following complete transection of the 25-μm-wide axon bundle using a single 800 nJ pulse, resulting in the severing of all axons in the track. The initial defect produced by the 800nJ pulse measures 50 μm across (Fig. 6b) and is roughly twice the size of the defect produced by the 400nJ pulse. Similar to the partially injured axon bundles, neurite dieback begins immediately following injury, and a bolus of neurons is formed which pulls back from the injury site on both the proximal and distal ends, identified by arrows in Fig. 6c. Within 1 h post-injury, distinct growth cones are seen to emerge from the proximal neurite segments (arrow, Fig. 6d).

Quantification of Axonal Dieback and Regeneration in Standard Media

Dieback and regeneration following laser-induced injury were quantitatively measured for both the partial and complete axotomies. A total of 12 tracks were monitored in each group to quantify the proximal and distal dieback distances following laser-induced injury at 30 min intervals for 2 h. Fig. 7a shows the post-injury distance of the closest axons on both proximal (positive) and distal (negative) sides measured laterally from the site of laser irradiation for both complete and partial axotomies. These measurements demonstrate that the proximal and distal distances from the injury site are roughly equal. Fig. 7b quantifies the distance of neurite dieback in response to the laser induced injury. Here we measured the distance from the site of laser focus to the start of the ‘bolus’ of neurites that are pulling away from the injury site at both the proximal and distal ends (shown in Fig. 5c). Again we see that the proximal and distal dieback distances from the site of laser focus are roughly

equal. Interestingly, while the spatial extent of dieback immediately following injury is shorter for the partial axotomies, within 2 h the dieback distances are equal for the partial and complete axotomies on both proximal and distal segments.

Axonal Response to Partial and Complete Transection in Media with EGTA

Previous studies have shown that calcium influx at the site of the injury plays a role in axonal dieback. To assess whether calcium is important for the dieback shown here, experiments were carried out in low calcium media.6 mM EGTA was added to the culture media 1 h prior to laser-induced injury to reduce the extracellular [Ca^{2+}] to below 0.3 μM[20]. Axonal dieback and regeneration of the proximal and distal segments were quantitatively measured in both partial and complete axotomy experiments under conditions of low extracellular [Ca^{2+}] with 15 tracks in each group. Fig. 8 shows the initial neurite response to a partial defect created in a 25-μm-wide axon bundle using a single 400 nJ pulse under standard culture conditions (Fig. 8a–c) compared to a sample in EGTA supplemented media (Fig. 8d–f). At 1 min following the laser microbeam injury there is little difference between size of the defect or appearance of the injured axons when comparing the result produced in standard culture media with that produced under conditions of reduced extracellular [Ca^{2+}] (compare Fig. 8a with 8d). However, within 30 min, neuritic dieback has commenced in the standard sample and a bolus of neurons has formed on the proximal and distal segments (arrows, Fig. 8b). In the EGTA supplemented sample, a bolus of neurons has also formed on either side of the defect, but the bolus does not retract from the site of injury and is marked by vacuolation accompanied by beading and blebbing in both the proximal and distal segments (arrows, Fig. 8e). Within 1.5 h, the neurites in the standard sample have demonstrated further dieback in the proximal segment and growth cones can be seen emerging across the injured site (arrow, Fig. 8c). By contrast, no dieback has occurred in the reduced-calcium sample. Instead, the axons exhibit further blebbing and degeneration with no sign of the formation of new growth cones (Fig. 8f).

The time-lapse images were measured for 2 h to quantify the dieback and regeneration dynamics in the control and reduced calcium samples. Fig. 9a depicts the distance between the closest axons and the site of laser focus for the partial defects. While the initial defect is slightly larger in the reduced-calcium samples, the control samples show an increased pull back from the site of injury within 60 min and begin the regrowth process after the first hour. By contrast, the distance between axons in the reduced calcium samples show a slight but steady decrease. However, this is due to the swelling and blebbing (see Fig. 8f) rather than axonal regeneration marked by the emergence of growth cones.

The extent of axonal dieback was also quantified by measuring the distance of the closest edge of the bolus of neurites that forms after the laser-induced injury. Fig. 9b provides a comparison of the dieback distance of the proximal and distal segments of the control and reduced calcium samples. The dieback distances of the proximal and distal segments in both groups are equal. However, we see that addition of EGTA essentially eliminates dieback of the proximal and distal axons.

In addition to the partial defect data described above, we examined both the initial dieback response and subsequent regeneration for up to 8 h for complete laser-induced axotomy in EGTA supplemented media. Fig. 10 provides a comparison of the neurite response to complete axotomy in standard cell culture conditions (Fig. 10a–10e) vs. that in calcium-reduced media (Fig. 10f–10j). The bolus of neurons that forms within 1 h (arrows, Fig. 10b–10e) appears to be absent in the reduced calcium culture (Fig. 10g–10j). Both cultures exhibit growth cones emerging from the proximal end within 3 h (Fig. 10c, 10h) and these axons bridge the gap of the defect to the distal end within 5 h (Fig. 10d, 10i). However, the extent of dieback and axonal regrowth is greatly reduced in the absence of calcium. Under

reduced calcium conditions, vacuolation accompanied by beading and blebbing is observed in both proximal and distal segments of individual neurites as early as 1 h (arrows, Fig. 10g). After 8 h, the axons that have crossed the gap in the calcium-reduced media appear to be thinner and less robust than those formed under standard culture conditions (Fig. 10e, 10j). Another interesting observation is that on occasion a single axon remained intact following laser injury as seen in Fig. 10a. In such cases

The dieback of both the proximal and distal segments was quantitatively monitored after complete laser-axotomy for up to 2 h. Fig. 11a illustrates the spatial extent of neurite dieback as measured by the distance between the closest edge of the proximal bolus to the closest edge of the distal bolus in the 12 control and 15 EGTA samples. Although the initial defect is roughly the same size in both samples 1 min following injury, the defect in the reduced calcium samples remains stationary, whereas the control samples demonstrate neurite dieback to a distance twice as large as the initial defect. To examine this further the distances of the closest proximal and distal neurons to the site of laser-induced injury was also measured and shown in Fig. 11b. The samples in reduced calcium media display very little dieback or subsequent regrowth. By contrast, the samples in standard culture media exhibit a larger spatial extent of injury in both the proximal and distal segments, and also enhanced axonal regeneration over a 2 h period.

Discussion

We have demonstrated the integrated use of picosecond laser microbeams and microfluidic cell culture to examine the injury and regeneration of linearly-oriented axonal bundles. Single exposures of highly-focused picosecond laser radiation achieve localized axonal injury with micrometer spatial resolution within the actively growing bundles. The zones of axonal injury are created by the formation of a laser-induced plasma followed by the emission of a pressure shock wave and cavitation bubble formation, expansion, and collapse[21,22,25]. Previous studies utilizing highly focused laser microbeam irradiation have demonstrated that cellular injury is due to direct vaporization by the plasma together with the mechanical shear stresses associated with the cavitation bubble expansion and/or collapse[21–25]. We performed time-resolved photography of the axonal injury process on the nanosecond and microsecond time-scale to confirm that this basic sequence of processes also holds for the injury of the axon bundles. The microfluidic design achieves spatial organization of these bundles using the biochemical cues provided by alternating strips of aggrecan and poly-L-lysine (PLL) that enables the study of these linearly oriented bundles of neurites in an environment separated from their respective cell bodies. Finally, we used time-lapse microscopy and image analysis to examine both proximal and distal segments of the injured axon and directly measure the sequential changes in neuritic response including initial dieback, degeneration, and regeneration. These dynamics were examined under standard cell culture conditions as well as in the presence of EGTA to reduce the extracellular [Ca^{2+}].

Integration of microfluidic cell culture and laser microbeam irradiation

The proposed integration of microfluidic cell culture with laser microbeam laser irradiation offers several advantages over other in vitro models of axonal injury[1–3]. First, the microfluidic approach allows explicit and precise manipulation of the spatial organization of CNS neurons. The use of alternating strips of aggrecan and PLL in the microfluidic cell culture confines the neurites to specific regions and also polarize their growth to allow anterograde and retrograde directions to be clearly defined by the directionality of the growing bundles. Second, picosecond laser microbeam irradiation produces precise and reproducible zones of axonal injury within the bundles independently from their respected cell bodies. By varying laser pulse energy, a single laser microbeam exposure can produce

partial or complete transection (Fig. 4a,b) while preserving both the proximal and the distal segments of the transected neurites. Moreover, the lower intensities associated with the use of picosecond exposures limits the cellular injury to acute effects produced by photothermal and photomechanical mechanisms without the photochemical effects associated with femtosesond exposures that may produce reactive oxygen species or direct damage of biomolecules[14]. Third, unlike other models of traumatic neuronal injury in which the integrity of the underlying matrix is invariably compromised[4] the preservation of the underlying aggrecan matrix is an essential and reliable characteristic of our model. Finally, unlike animal models, this *in vitro* model is free from effects of many systemic and homeostatic influences, and allows control of the extracellular environment.

Degenerative and Regenerative Changes Following Neurite Transection

Cajal[26] first described the process post-traumatic retrograde degeneration or dieback that has since been recognized as a distinct characteristic of many in vitro axonal injury models[27] and is observed in our model microfluidic cell culture system. The use of 400 and 800 nJ pulse energies provide for the creation of both partial and complete transections (Figs. 4a&b, respectively). Under standard culture conditions retrograde regression was observed to commence immediately following injury and was complete within 30 min for both partial and complete neurite transections. Our time-resolved imaging study revealed that axonal injury occurs within a few microseconds following laser microbeam irradiation. Hence, the observed degenerative alterations, which occur on much larger time scales (1–60min), can be interpreted as a secondary but direct consequence of a neuro-chemical or cellular cascade set into motion by the initial, primary laser-induced injury. The spatial extent of these changes was successfully quantified by time-lapse microscopy. While the initial proximal and distal distances from the injury site were roughly equal in both partial and complete transections (Fig. 7a,b), the degenerative events in the distal neuritic segments became more conspicuous 1 h following the laser-induced injury. As early as 1–2 h following injury vacuolation and some blebbing is clearly observed in the distal segments of neuritis disconnected from the cell bodies (Fig. 8b,c), while the reduced calcium conditions caused more severe vacuolation and blebbing in both the proximal and distal segments (Fig. 8e,f).

Comparable changes have been described in animal models of spinal cord injury as well as in humans[28]. Significant morphological changes are apparent in the distal segments of the tracks, and are characteristic of degenerating neurites in response to a variety of insults, including exposure to profound hypothermia, hydrogen peroxide, or a variety of calcium ionophores[29,30]. While degenerative changes were arrested in the proximal neuritic segment, the degenerating distal neurite continued to withdraw from the immediate injury site, and eventually detached from the matrix bed.

Another consistent feature of our model was the process of neurite regeneration following transection. This post-injury process is clearly differentiable from normal growth during maturation of the cultures and commenced approximately 2h following the completion of the dieback process. Figs. 5 and 6 demonstrate the emergence of distinct growth cones from the proximal neuritic segments in standard culture media. Within 3–5 h, a uniform front of regenerating axons could be seen beginning to cross the site of injury. The degenerative distal neurites continued to withdraw and posed no barrier to the growing front of regenerating axons, which were able to eventually regrow and traverse the injury site.

Effect of EGTA on Injury Dynamics and Regeneration

Extracellular calcium influx into the amputated axons has been postulated as the hallmark of the degenerative changes following axonal trauma[20]. To demonstrate the potential utility of our method as a conduit for more in depth analysis of this phenomenon, we added 6mM of

EGTA as a model drug to chelate extracellular calcium to alleviate the degenerative changes in partially and completely transected bundles.

Our results demonstrate that under standard culture conditions, axotomy leads to a degeneration wave that propagates in the retrograde direction along the proximal axon and the anterograde direction along the distal isolated segments, on a time scale of a few minutes. The fact that neurite degeneration of both ends occurs on a time scale of minutes (Fig. 8) implies that the initial cascade triggered by axotomy is in fact of a local nature and independent of the cell body. We found that the immediate proximal & distal dieback distances from the site of laser focus were roughly equal, under both standard and reduced Ca^{2+} conditions. In other words, the initial morphological alterations experienced by the proximal and distal cut ends in standard and reduced calcium media appear identical. However, within 30–60 min post ablation, clear differences begin to emerge. Quantification of the neurite dieback revealed that, unlike the neurites grown in standard culture media that exhibit a larger spatial extension of injury on both the proximal and distal segments, the reduced calcium samples displayed very little dieback. Whereas distinct growth cones emerge from the proximal neurite segments in control samples (arrow, Fig. 8c), only aberrant structures are formed by the proximal and isolated distal segments of the reduced-calcium sample, which subsequently fail to grow or develop.

These observations are consistent with numerous studies[20,31,32] that demonstrate that axotomy triggers a cascade of events leading to structural reorganization on both sides of the cut. The rupture of the plasma membrane leads to a calcium influx for both proximal and distal cut ends, where transient $[Ca^{2+}]_i$ gradients have shown to be formed over a few hundred micrometers along both cut ends. The elevated $[Ca^{2+}]_i$ on both sides of the cut induce disassembly of microtubules. These gradients relax within minutes of axotomy as soon as a membrane seal is formed (1–5 min). The cascade of events that follows axotomy has been further subdivided into initial events that unfold in parallel as mirror images in the proximal and distal cut ends, and delayed phases in which the responses of the two cut ends diverge. Initially, axotomy leads to highly orchestrated restructuring cascade along an axonal segment of 50–150 μm, stretching proximally and distally away from the site of transection. This phase occurs along both proximal and distal segments on a time scale of tens of minutes. Our model system clearly displays these characteristic morphological traits and time scales of the injury and regeneration dynamics.

Correspondence of in vitro Model Results to in vivo Models

Comparable distinct morphological features have been described in *in vivo* animal models of spinal cord injury (SCI) as well as in human head and spinal cord injuries. For example, the vacuolation of individual neurites and neuritic fascicles along their length (Fig. 5,6,8) have also been observed *in vivo*[28]. The reproduction of such distinct morphological features in our *in vitro* model, such as vacuolation of individual neurites and neuritic fascicles along their length, indicates of the suitability of this in vitro model to examine events of axonal injury that occur *in vivo*. The post traumatic retrograde regression is a feature that has since been recognized as a distinct trait of many in vitro axonal injury models[27] and one that our model of injury distinctively and reliably displays.

An important attribute of the microfluidic model system injury model, is the hostile and inhibitory local environment of the CNS post-injury. Unlike injured neurites *in vivo*, a tissue culture dish environment lacks the glial scar, which inhibits the growth of regenerating neurites. An active molecular component of the glial scar, Aggrecan, has been integrated into our injury model. This allows pre- and post-traumatic alignment of the proximal and distal neuritic front in a manner that facilitates quantification of neurite outgrowth. These

results are expected to be relevant to the *in vivo* situation. These results demonstrate that laser microbeam-irradiated CNS neurites retain their ability to regenerate.

Conclusion

The integration of the pulsed laser microbeam irradiation with microfluidic neuronal cell culture and time-lapse microscopy allows the study of dynamics of axonal injury and regrowth under controlled conditions. Our utilization of single picosecond laser pulses to create precise, reproducible, and localized injury to neuronal processes permits axons to be severed without injury to the cell bodies or the underlying matrix. Furthermore, time-lapse microscopy allows examination of both proximal and distal segments and quantitative image analysis provides direct measurement of sequential changes in neurite response, such as dieback, anterograde degeneration, and regeneration. Adjustment of the laser microbeam pulse energy allows the generation of partial or complete transection of the axon bundles using a single exposure. Moreover, this model system preserves the distal segments of the transected neurites and provides the opportunity to study the fate and the anterograde (Wallerian) degeneration of the severed neuritic fragments. Our model system allows the examination of several utilizes neurite bundles (25–35 neurites per track) simultaneous and is provides a distinct improvement over previous models of *in vitro* axonal injury that are limited to the study of one or two cells (or processes)[33]. This method can facilitate the rapid screening and discovery of biomolecules that may affect axonal regeneration and development of CNS neurons. Furthermore, this approach can be readily adapted by the spinal cord injury research community as a standard platform for comparison of results across laboratories.

Acknowledgments

Support provided by the National Institutes of Health via the Laser Microbeam and Medical Program P41 RR01192 and R01 EB04436, University of California Systemwide Biotechnology Research and Education Program GREAT Training Grant (#2006-12), and WCU (World Class University) program of the Korea Science and Engineering Foundation funded by the Ministry of Education, Science and Technology (R31-2008-000-10083-0). We thank Xona Microfluidics, LLC for technical assistance.

References

1. Quilty M, Gai W, Pountney DL, West AK, Vickers JC. Localization of alpha-, beta-, and gamma-synuclein during neuronal development and alterations associated with the neuronal response to axonal trauma. Exp Neurol. 2003; 182:195–207. [PubMed: 12821390]
2. Mandolesi G, Madeddu F, Bozzi Y, Maffei L, Ratto GM. Acute physiological response of mammalian central neurons to axotomy: ionic regulation and electrical activity. FASEB J. 2004; 18:1934–1936. [PubMed: 15451889]
3. Fayaz I, Tator C. Modeling axonal injury in vitro: injury and regeneration following acute neuritic trauma. J Neurosci Methods. 2000; 102:69–79. [PubMed: 11000413]
4. Mukhin A, Ivanova S, Knoblach SM, Faden AI. New in vitro model of traumatic neuronal injury: evaluation of secondary injury and glutamate receptor-mediated neurotoxicity. J Neurotrauma. 1997; 14:651–663. [PubMed: 9337127]
5. Campenot R. Development of sympathetic neurons in compartmentalized cultures.1. Local control of neurite growth by nerve growth factor. Dev Biol. 1982; 93:1–12. [PubMed: 7128926]
6. Taylor A, Blurton-Jones M, Rhee SW, Cribbs DH, Cotman CW, Jeon NL. A microfluidic culture platform for CNS axonal injury, regeneration and transport. Nature Meth. 2005; 2:599–605.
7. Park J, Vahidi B, Taylor AM, Rhee SW, Jeon NL. Microfluidic culture platform for neuroscience research. Nat Protoc. 2006; 1:2128–2136. [PubMed: 17487204]
8. Park J, Vahidi B, Kim HJ, Rhee SW, Jeon NL. Quantitative Analysis of CNS axon regeneration using a microfluidic neuron culture device. Biochip J. 2008; 2:44–51.

9. Yanik M, Cinar H, Cinar HN, Chisholm AD, Jin YS, Ben-Yakar A. Neurosurgery-Functional regeneration after laser axotomy. Nature. 2004; 432:822. [PubMed: 15602545]
10. Yanik M, Cinar H, Cinar HN, Gibby A, Chisholm AD, Jin Y, Ben-Yakar A. Nerve regeneration in C. elegans after femtosecond laser axotomy. IEEE J Sel Top Quantum Electron. 2006; 12:1283–1291.
11. Bourgeois F, Ben-Yakar A. Femtosecond laser nanoaxotomy properties and their effect on axonal recovery in C-elegans. Opt Express. 2007; 15:8521–8531. [PubMed: 19547186]
12. Rao GN, Kulkarni SS, Koushika SP, Rau KR. In vivo nanosecond laser axotomy: cavitation dynamics and vesicle transport. Opt Express. 2008; 16:9884–9894. [PubMed: 18575558]
13. Tirlapur U, Konig K. Cell biology-Targeted transfection by femtosecond laser. Nature. 2002; 418:290–291. [PubMed: 12124612]
14. Vogel A, Noack J, Huttman G, Paltauf G. Mechanisms of femtosecond laser nanosurgery of cells and tissues. Appl Phys B. 2005; 81:1015–1047.
15. Vahidi B, Park J, Kim HJ, Jeon NL. Microfluidic-based strip assay for testing the effects of various surfact-bound inhibitors in spinal cord injury. J Neurosci Methods. 2008; 170:188–196. [PubMed: 18314199]
16. Ivins KJ, Bui ETN, Cotman CW. Beta-amyloid induces local neurite degeneration in cultured hippocampal neurons: Evidence for neuritic apoptosis. Neurobiol Dis. 1998; 5:365–378. [PubMed: 10069579]
17. Taylor A, Rhee S, Tu CH, Cribbs DH, Cotman CW, Jeon NL. Microfluidic multicompartment device for neuroscience research. Langmuir. 2003; 19:1551–1556. [PubMed: 20725530]
18. Kim E, Xia Y, Whitesides GM. Polymer microstructures formed by molding in capillaries. Nature. 1995; 376:581–584.
19. Kim E, Xia YN, Whitesides GM. Micromolding in capillaries: Applications in materials science. J Am Chem Soc. 1996; 118:5722–5731.
20. Schlaepfer W, Bunge R. Effects of calcium-ion concentration on degeneration of amputated axons in tissue culture. J Cell Biol. 1973; 59:456–470. [PubMed: 4805010]
21. Rau KR, Guerra A, Vogel A, Venugopalan V. Investigation of laser-induced cell lysis using time-resolved imaging. Appl Phys Lett. 2004; 84:2940–2942.
22. Rau KR, Quinto-Su P, Hellman AN, Venugopalan V. Pulsed laser microbeam-induced cell lysis: Time-resolved imaging and analysis of hydrodynamic effects. Biophys J. 2006; 91:317–329. [PubMed: 16617076]
23. Hellman A, Rau K, Yoon HH, Venugopalan V. Biophysical response to pulsed laser microbeam-induced cell lysis and molecular delivery. J Biophotonics. 2008; 1:24–35. [PubMed: 19343632]
24. Quinto-Su PA, Lai H, Yoon HH, Sims CE, Allbritton NL, Venugopalan V. Examination of laser microbeam cell lysis in a PDMS microfluidic channel using time-resolved imaging. Lab Chip. 2008; 8:408–414. [PubMed: 18305858]
25. Venugopalan V, Guerra A III, Nahen K, Vogel A. Role of laser-induced plasma formation in pulsed cellular microsurgery and micromanipulation. Phys Rev Lett. 2002; 88:078103. [PubMed: 11863944]
26. Cajal, SR. Degeneration and regeneration of the nervous system. Oxford Univ. Press; London: 1928.
27. Morrison B, Saatman KE, Meaney DF, McIntosh TK. In vitro central nervous system models of mechanically induced trauma: A review. J Neurotrauma. 1998; 15:911–928. [PubMed: 9840765]
28. Tator CH. Update on the pathphysiology and pathology of acute spinal-cord injury. Brain Pathol. 2005; 5:407–413. [PubMed: 8974623]
29. Hinshaw DB, Miller MT, Omann GM, Beals TF, Hyslop PA. A cellular model of oxidant-mediated neuronal injury. Brain Res. 1993; 615:13–26. [PubMed: 8364721]
30. Emery DG, Lucas JH. Ultrastructural damage and neuritic beading in cold-stressed spinal neurons with comparisons to NMDA and A23187 toxicity. Brain Res. 1995; 692:161–173. [PubMed: 8548300]

31. Erez H, Malkinso G, Pragel-Khoutorsky M, De Zeeuw CI, Hoogenraad CC, Spira ME. Formation of microtubule-based traps controls the sorting and concentration of vesicles to restricted sites of regenerating neurons after axotomy. J Cell Biol. 2007; 176:497–507. [PubMed: 17283182]

32. Erez HG, Spira ME. Local self-assembly mechanisms underlie the differential transformation of the proximal and distal cut axonal ends into functional and aberrant growth cones. J Comp Neurol. 2008; 507:1019–1030. [PubMed: 18092341]

33. Lucas JH, Kirkpatrick JB, Gross GW. A photoetched cell relocation matrix for long-term, quantitative observations of selected individual neurons in culture. J Neurosci Methods. 1985; 14:211–219. [PubMed: 3900593]

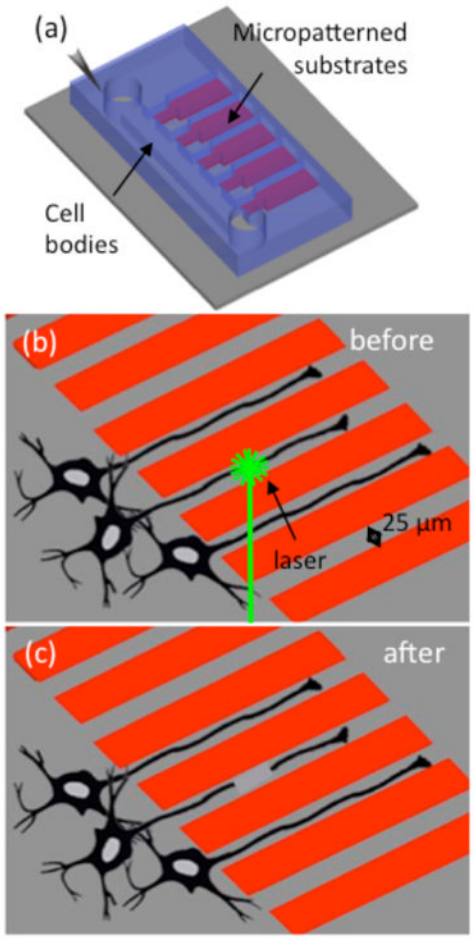

Figure 1.
(a) Microfluidic-based culture platform using surface micropatterning. (b) Before and (c) after illustrations of laser induced axotomy to provide precise damage to selected neurons while preserving both the proximal and distal segments of transected axons and leaving the cell bodies intact.

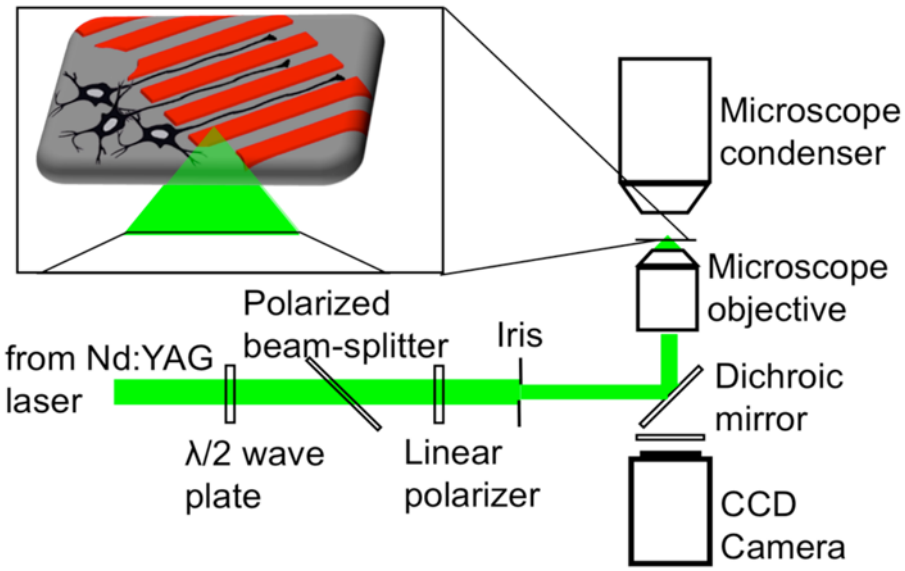

Figure 2.
Experimental setup for laser microbeam axotomy and time-lapse microscopy.

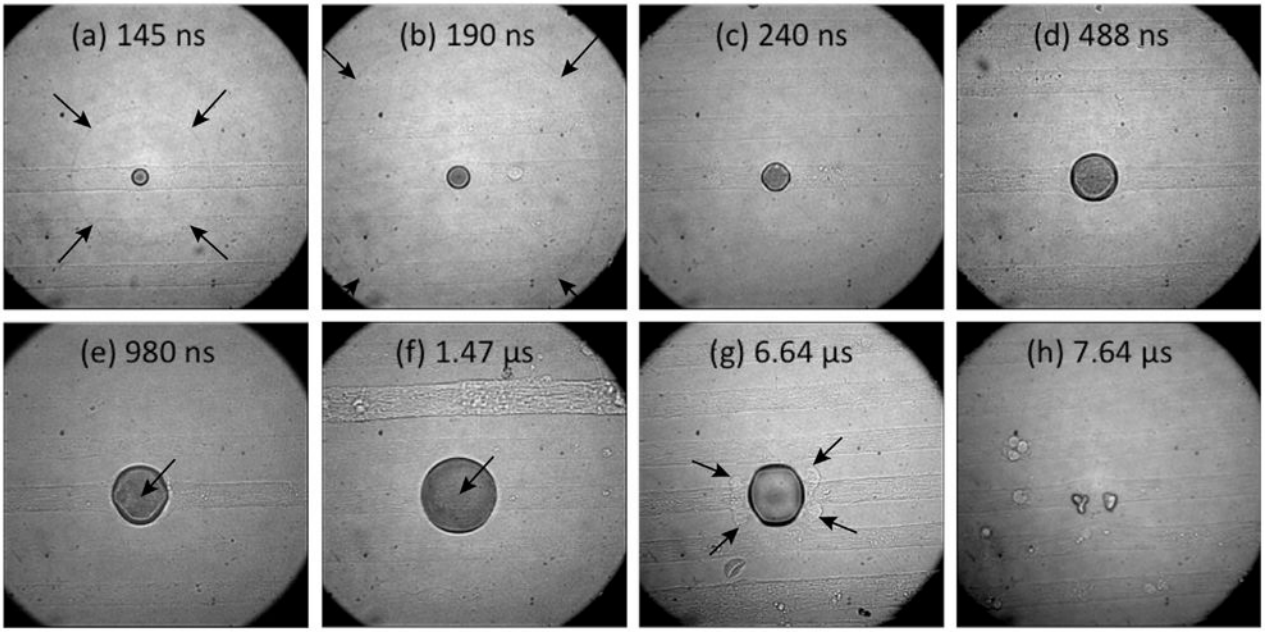

Figure 3.
Time-resolved image series of laser axotomy of 25-μm-wide bundles following irradiation with a single 180 ps duration, 0.5 μJ laser microbeam exposure. Shock wave propagation (arrows, a,b), cavitation bubble expansion (a–f) and collapse (g–h) and development of the axonal injury processes are clearly seen. Axon severing inside the bubble (arrows, e, f), and deformation of axon bundles near the outside edge of the bubble (arrows, g) are also shown. Image times are as marked.

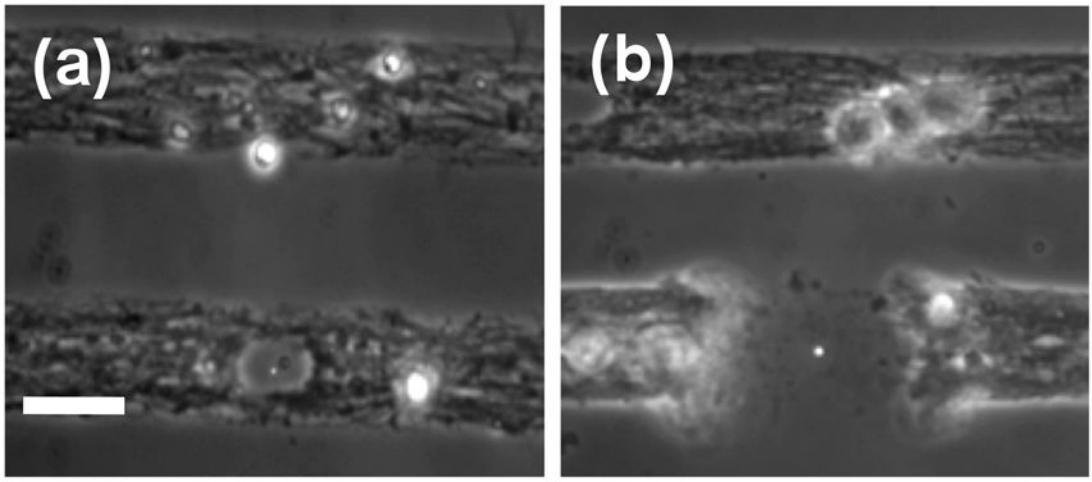

Figure 4.

Axotomy of 25 μm axon strips using a single 180 ps laser pulse. Axotomy was performed on the lower strip, leaving the neighboring upper strip unaffected. Images taken 1 min following laser pulse delivery: (a) partial and (b) complete transections, using E_p=400 nJ and 800 nJ, respectively. Scale bar = 25 μm.

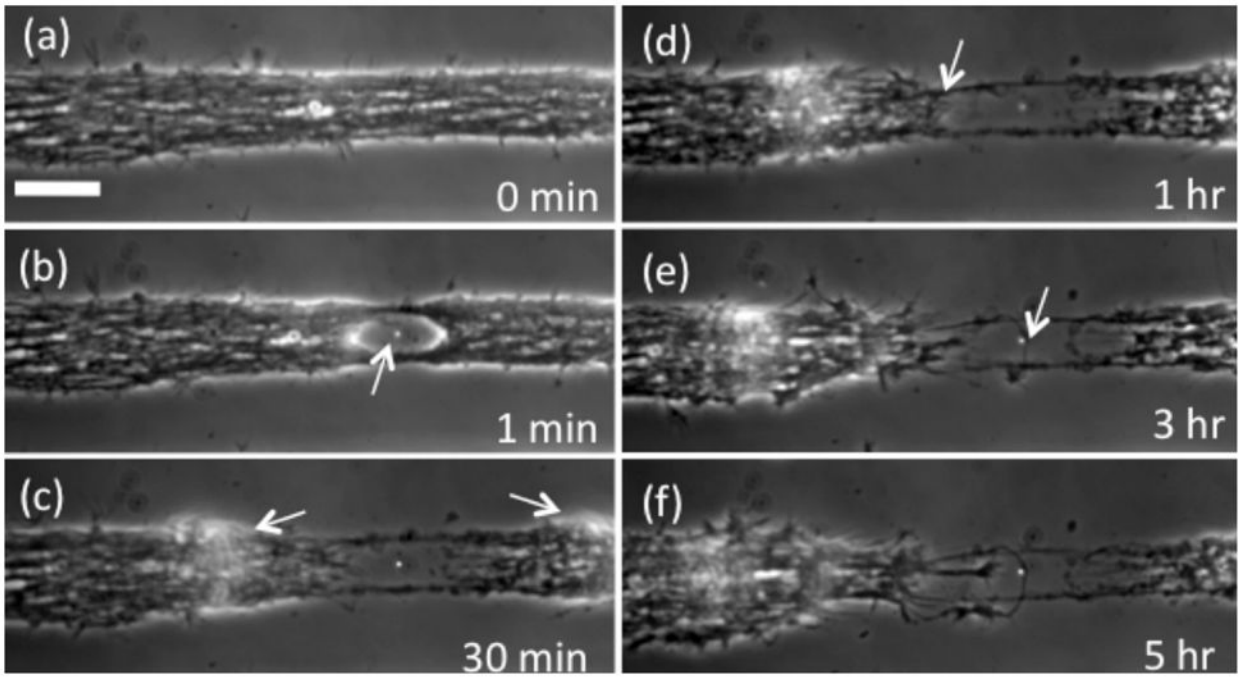

Figure 5.

Partial defect created in a 25 μm-wide axon bundle using a single 400 nJ pulse. Proximal and distal segments are on the left and right, respectively. (a) Before axotomy, (b) 1 min following axotomy with arrow indicating site of laser focus. (c) initial dieback of axons observed (arrows) (d) growth cones begin to emerge from the proximal side of the device (arrow). (e, f) Growth cones have emerged and begin to regenerate across the injury site. Scale bar = 25 μm.

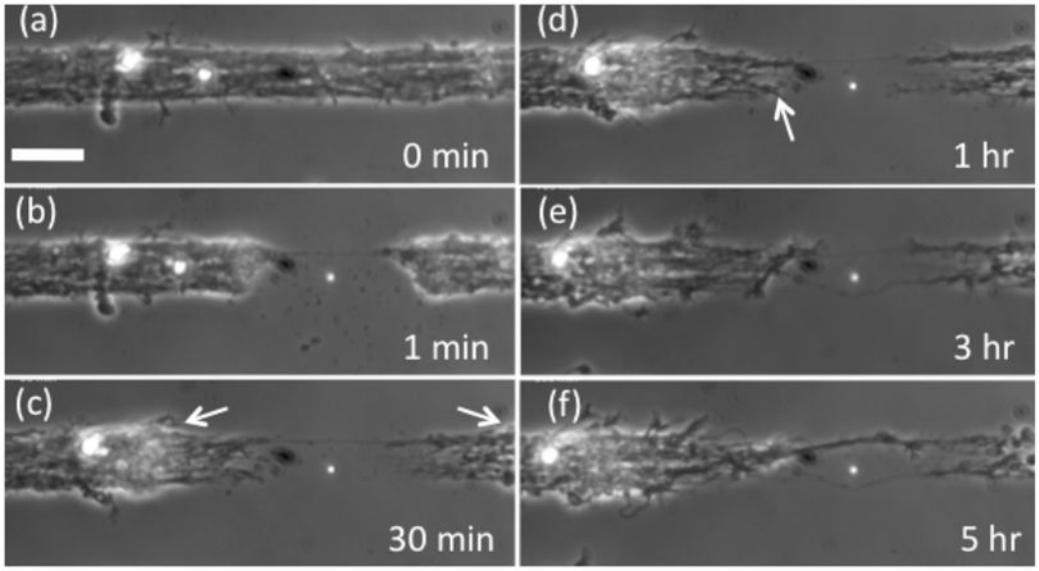

Figure 6.
Complete transection of a 25 μm-wide axon bundle produced by a single 800 nJ pulse. (a) Before axotomy; (b) 1 min following axotomy; (c) initial dieback of axons observed (arrows); (d) growth cones begin to emerge from the proximal side of the device (arrow); (e, f) Growth cones have emerged and begin to regenerate across the injury site. Scale bar = 25 μm.

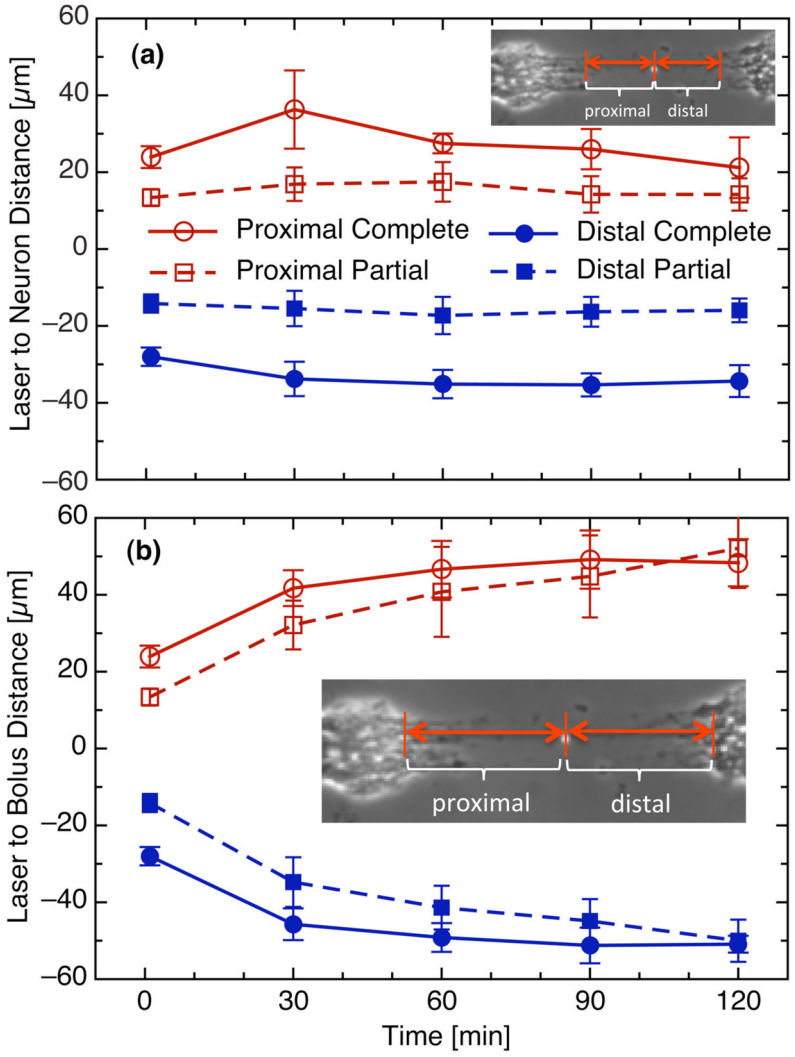

Figure 7.

Evolution of neuritic injury and regeneration for partial (dashed lines) and complete (solid lines) defects produced following laser microbeam irradiation of 25 μm-wide axon bundles. Site of laser delivery = 0 μm. (a) distance between the closest proximal/distal axon to laser focus. (b) Distance between the closest edge of the neuron 'bolus' and the site of laser irradiation.

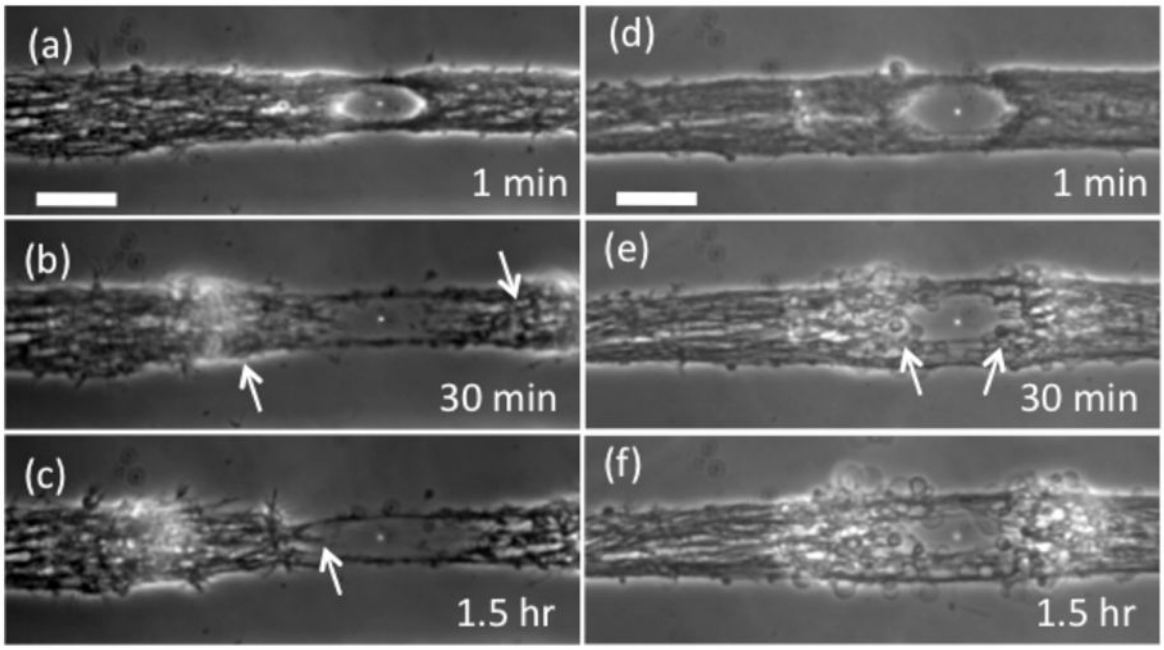

Figure 8.
Partial transection of a 25 μm-wide axon bundle following a single 400 nJ pulse. (a–c) Standard culture media and (d–f) EGTA supplemented media. Scale bar = 25 μm.

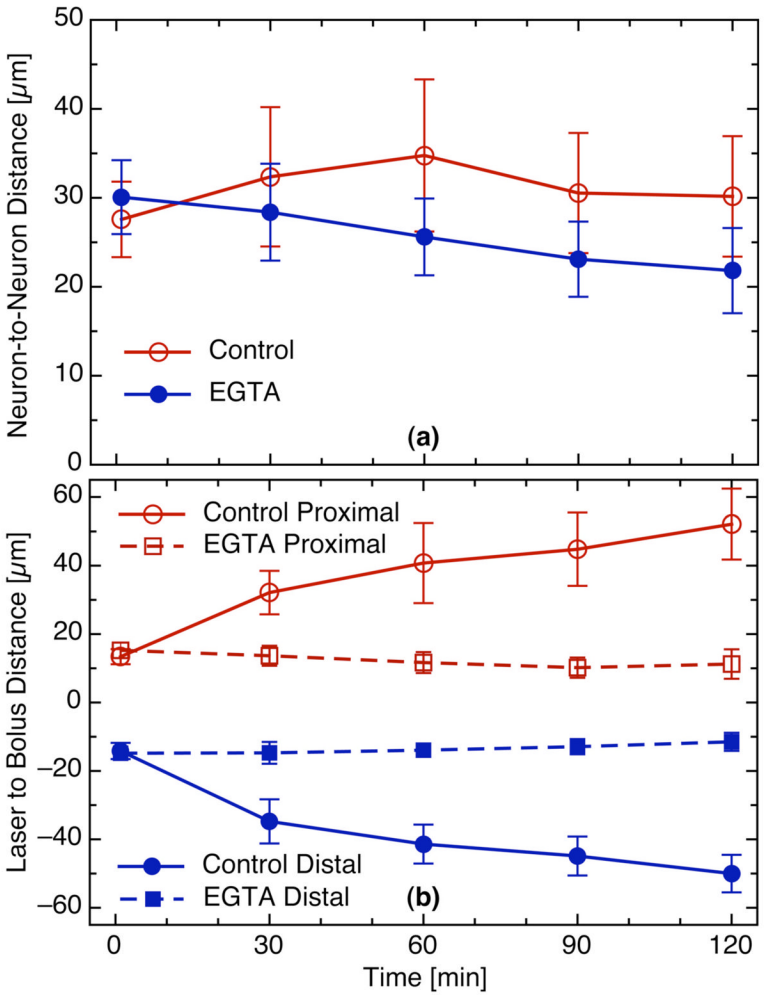

Figure 9.

Evolution of partial injury resulting from a single 400 nJ laser exposure in standard culture and reduced calcium media. (a) Distance across the partial defect measured from the closest proximal and distal axons to the site of laser irradiation. (b) Distance between the dieback bolus of neurons on the proximal (solid lines) and distal (dashed lines) segments.

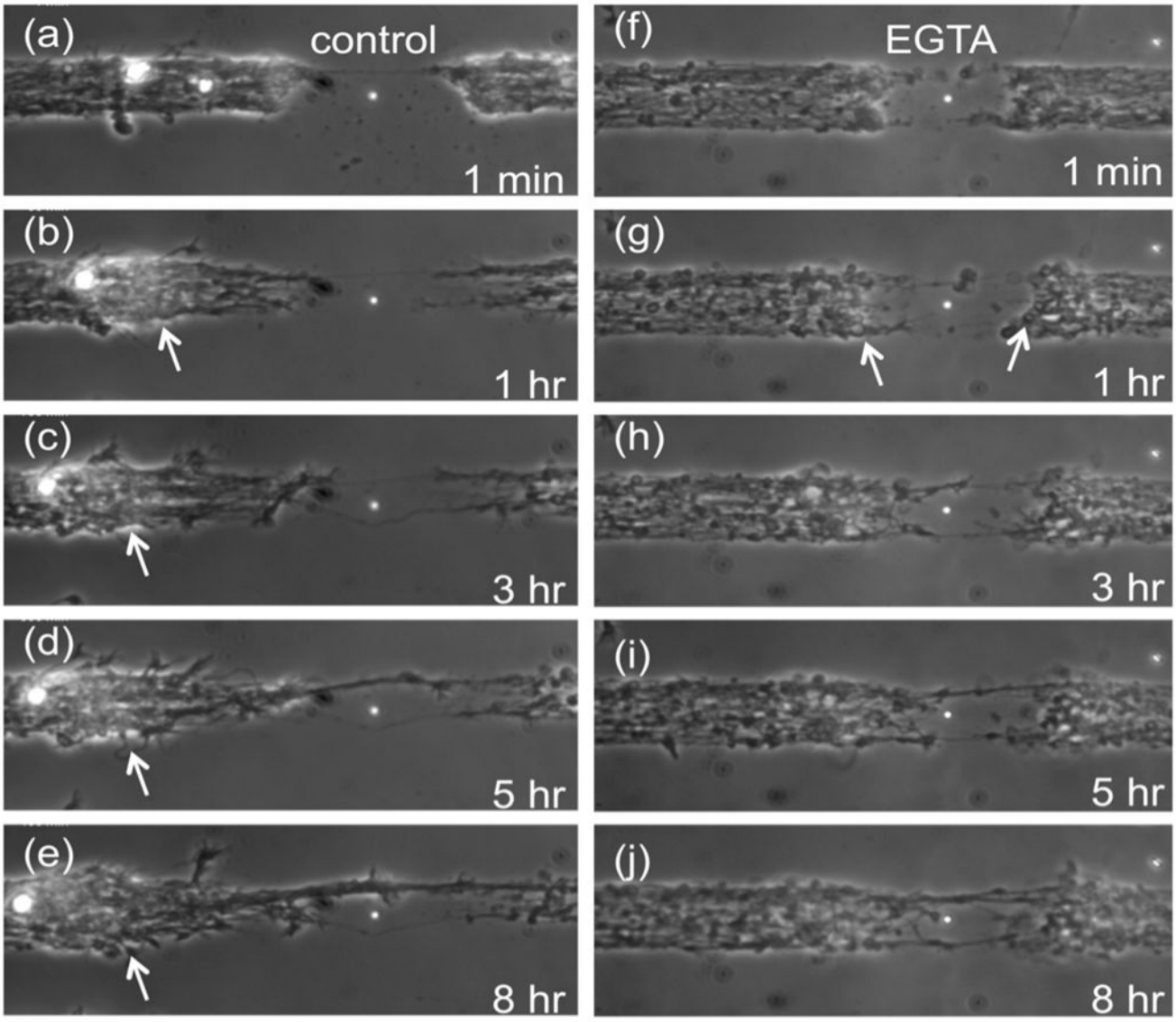

Figure 10.
Complete transection of a 25 μm-wide axon bundle using a single 800 nJ pulse. (a–e) Standard culture media and (f–i) EGTA supplemented media.

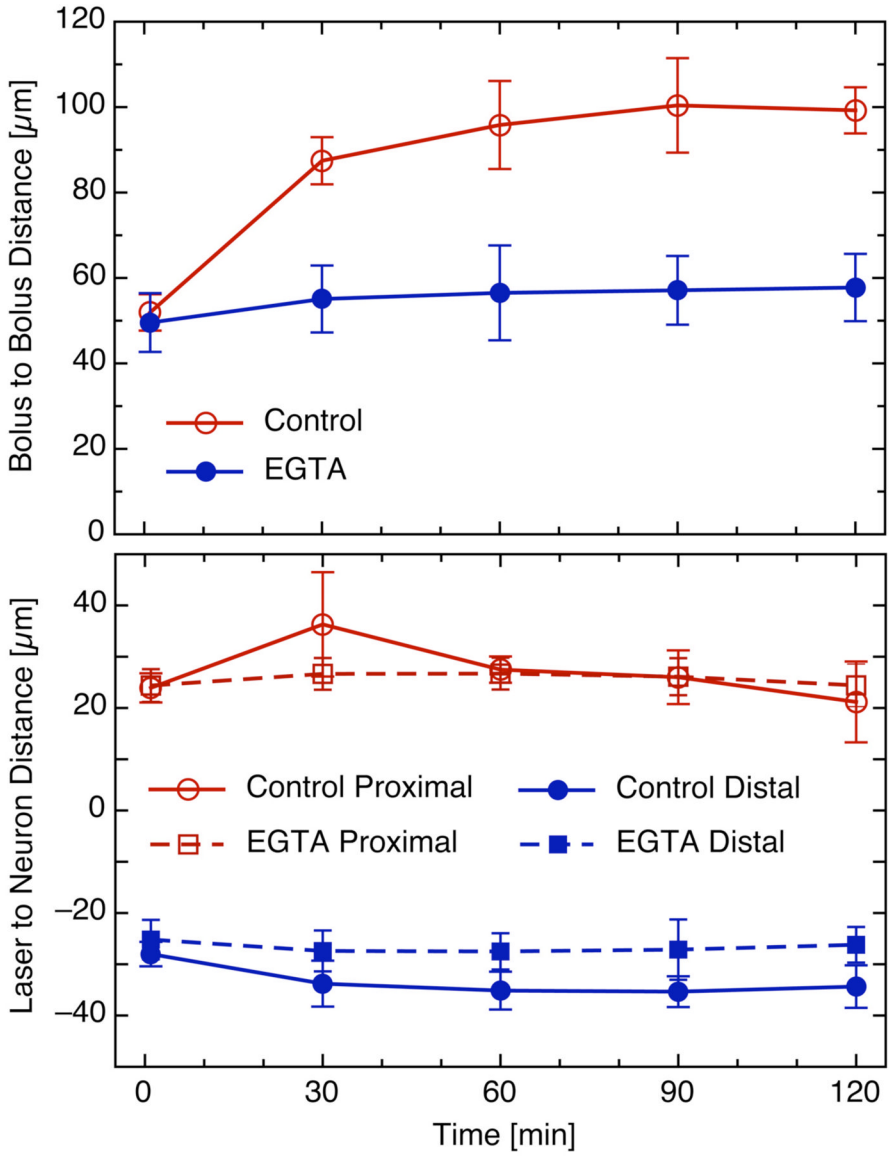

Figure 11.
Neurite dieback following complete axonal transection using a single 800 nJ pulse. (a) Distance between the closest edge of proximal bolus to the closest edge of the distal bolus; (b) distance between proximal (solid lines) and distal (dashed lines) neurons to site of laser focus.